Yahui Zhang
BioMfG Laboratory,
Center for Computer-Aided Design,
The University of Iowa,
Iowa City, IA 52242;
Department of Mechanical and
Industrial Engineering,
The University of Iowa,
Iowa City, IA 52242

Yin Yu
BioMfG Laboratory,
Center for Computer-Aided Design,
The University of Iowa,
Iowa City, IA 52242;
Department of Biomedical Engineering,
The University of Iowa,
Iowa City, IA 52242

Ibrahim T. Ozbolat[1]
BioMfG Laboratory,
Center for Computer-Aided Design,
The University of Iowa,
Iowa City, IA 52242;
Department of Mechanical and
Industrial Engineering,
The University of Iowa,
Iowa City, IA 52242
e-mail: ibrahim-ozbolat@uiowa.edu

Direct Bioprinting of Vessel-Like Tubular Microfluidic Channels

Despite the progress in tissue engineering, several challenges must be addressed for organ printing to become a reality. The most critical challenge is the integration of a vascular network, which is also a problem that the majority of tissue engineering technologies are facing. An embedded microfluidic channel network is probably the most promising solution to this problem. However, the available microfluidic channel fabrication technologies either have difficulty achieving a three-dimensional complex structure or are difficult to integrate within cell printing process in tandem. In this paper, a novel printable vessel-like microfluidic channel fabrication method is introduced that enables direct bioprinting of cellular microfluidic channels in form of hollow tubes. Alginate and chitosan hydrogels were used to fabricate microfluidic channels showing the versatility of the process. Geometric characterization was performed to understand effect of biomaterial and its flow rheology on geometric properties. Microfluidic channels were printed and embedded within bulk hydrogel to test their functionality through perfusion of cell type oxygenized media. Cell viability experiments were conducted and showed great promise of the microfluidic channels for development of vascular networks. [DOI: 10.1115/1.4024398]

Keywords: *microfluidic channels, bioprinting, tissue engineering*

1 Introduction

Although great progress has been made in biofabrication of tissue constructs over the past decades, the engineered constructs still have difficulty in biomimicking the functional thick tissues or organs, due to an inefficient media exchange rate [1]. Nonhomogeneous cell distribution and limited metabolic activities are often observed, since planted cells cannot get enough oxygen, growth factors and nutrients for their metabolic activities which are needed for maturation during perfusion. Microfluidic system integration has shown great potential to alleviate current limitations. Lee and his coworkers [2] have shown great difference in cell viability with or without an embedded microfluidic channel in hydrogel scaffolds. Ling et al. [3] demonstrated that microfluidic channels are capable of delivering sufficient nutrients to encapsulated cells, and higher cell viability resulted in the region closer to the microfluidic channel. In addition, microfluidic channel systems were not only able to provide media to maintain cell metabolic activities but also to delivered signals to guide cell activities.

To date, several methods have been used in microfluidic fabrication, including soft lithograph [3–5], photo-patterning [6–8], laser-based technologies [9,10], molding [11–13], and bioprinting [2,14–16]. However, due to their intrinsic characteristics, each of the above-mentioned technologies has its advantages and disadvantages. Soft lithography is the most popular method in microfluidic channel fabrication due to its low cost, accuracy, and reproducibility. Using soft lithography technology, Ling et al. [3] fabricated microfluidic cell-laden agarose hydrogel, which resulted in a significant increase in cell viability during media perfusion compared to static controls. Cuchiara et al. [4] developed a soft lithography process to fabricate a poly(ethylene glycol) diacrylate hydrogel microfluidic network. With media perfusion, encapsulated mammalian cells maintained a high viability rate in bulk hydrogel. However, soft lithograph is not a viable option for fabrication of complex three-dimensional (3D) constructs due to its cumbersome procedures. Despite their superior accuracy and repeatability, photo-patterning and laser-based methods may not be suitable for fabricating thick tissue constructs because of their limited light-penetrating depths in precursor solution. Offra et al. [6] proposed a focal laser photoablation capable of generating microstructures in transparent hydrogels. Cell behavior was successfully guided by the microchannel pattern. Molding is an inexpensive and scalable method, but complex 3D geometry is difficult to achieve and postprocedures are required after fabrication. In Ref. [12], Nazhat et al. used a molding method to incorporate unidirectionally aligned soluble phosphate-based glass fibers into dense collagen scaffolds. The diameters of the achieved microfluidic channels were around 30–40 μm, and a significant increase in cell viability was observed in the hydrogel sheets. Despite the plethora of work in microfluidic channel fabrication using the traditional methods, only a few researchers have developed strategies for bioprinting of microfluidic channels, where bioprinting can be defined as computer-controlled layer-by-layer bioadditive process enabling printing living cells precisely per predefined patterns [1]. Cell encapsulated biomaterials can be directly patterned onto substrate without any pretreating steps (such as mold or mask preparation). It offers several advantages, including precise control [16,17], automated fabrication capability [18,19], and feasibility of achieving complex shapes [15]. Zhao et al. [20] recently presented a methodology in bioprinting of perfused straight microfluidic channel structures in thick hydrogel. They created a temporary structure to form the hollow cavity which was then removed by a postprocess.

In this study, a novel bioprinting fabrication process is introduced, where vessel-like microfluidic channels can be directly printed in complex shapes without any need of pre/post processes.

[1]Corresponding author.

Manuscript received February 15, 2012; final manuscript received April 26, 2013; published online July 23, 2013. Assoc. Editor: Shaurya Prakash.

Microfluidic channels, in the form of hollow filaments, are directly printed by a pressure-assisted robotic system using hydrogels. We performed geometric characterization of microfluidic channels through studying multiple biomaterials and their dispensing rheology. Then, microfluidic channels were embedded in bulk hydrogel to evaluate their structural integrity and media perfusion capability. Further, we examined the media transportation capability of printed and embedded microfluidic channels by perfusing oxygenized cell culture media through patterned channels. A cell viability study was carried out to access the effect of perfusion on encapsulated cells.

2 Materials and Methods

2.1 Materials. Prior to making a hydrogel solution, sodium alginate powder (Sigma Aldrich, United Kingdom), chitosan powder (Sigma Aldrich, Iceland), and calcium chloride powder (Sigma Aldrich, United Kingdom) were treated with ultraviolet (UV) light for sterilization three times for a 30-minute cycle [16]. UV-sterilized sodium alginate was dissolved in deionized water to make 3%, 4%, 5%, and 6% (w/v) solutions. UV-sterilized chitosan was dissolved in 1.0 M acetic acid (Fluka Analytical, Germany) to make 2%, 2.5%, 3%, and 4% (w/v) solutions. Solutions were mixed with a magnetic stirrer (HANNA Instruments, Rhode Island, USA) until homogeneity was reached. Similarly, the crosslinking solution was prepared by dissolving UV-sterilized calcium chloride in ultrapurified water (InvitrogenTM Life Technologies, Carlsbad, CA) at 4% (w/v). 1.0 M sodium hydroxide (Fluka Analytical, Germany) is used to crosslink the chitosan solution.

2.2 Cell Preparation. In order to evaluate the efficiency of microfluidic channels for cell viability, we used cartilage progenitor cells (CPCs) [20,21] in our study. CPCs were cultured at 37 °C in 5% CO_2 in DMEM/F12 (1:1) supplemented with 10% fetal bovine serum (InvitrogenTM Life Technologies, Carlsbad, CA), 50 μg/μl L-ascorbate, 100 μg/μl penicillin, 100 μg/ml streptomycin, and 2.5 μg/μl Fungizone. Culture media was changed every other day. Cells were harvested until we achieved a sufficient amount for bioprinting. After harvesting, cells were centrifuged down and resuspended in 4% sodium alginate, and gently mixed with alginate solution by a vortex mixer to get uniform distribution. The cell seeding density used in this study was 2×10^6 cells/ml.

2.3 Biofabrication of Microfluidic Channels. The microfluidic channel fabrication system consisted of five parts: a single-arm robotic printer (EFD® Nordson, East Providence, RI); a homemade co-axial nozzle unit; a syringe pump (New Era Pump System Inc., Farmingdale, NY, East Providence, RI), which was used to dispense crosslinker; a liquid dispenser (EFD® Nordson), which was used to dispense biomaterial; and a computer that was used for robotic control. Figure 1(*a*) shows a representative model of the experiment setup developed in Pro/Engineer software. Two coaxial nozzle assemblies were used in this research: an assembly with 26 gauge (230 μm inner diameter (I.D.) (Integrated Manufacturing Solution, USA), 457 μm outer diameter (O.D.)) inner needle, and an 18 gauge (840 μm I.D., 1270 μm O.D.) outer needle used for the experiment in Sec. 3.2, and another assembly with a 23 gauge (330 μm I.D., 650 μm O.D.) inner needle and an 18 gauge (840 μm I.D., 1270 μm O.D.) outer needle used for the experiment in Sec. 3.3. Biomaterial and its crosslinker solutions were loaded separately into the coaxial nozzle unit. The coaxial nozzle assembly consisted of three parts: a feed tube, an outer tube, and an inner tube. A representative model of the coaxial nozzle with hydrogel and crosslinker solution flow paths is demonstrated in Fig. 1(*b*). During the printing process, the coaxial unit was mounted on the single-arm robot, which was controlled by a computer. Hydrogel solutions were pumped into the feed tube, which was used to feed hydrogel solution (alginate or chitosan) into the space formed between the outer and inner tubes. Hydrogel solution flowed through this space and dispensed out from the outer tube tip. Crosslinker was dispensed through inner tube. When the two solutions contacted, crosslinking (or gelation) started, and a tubular gel was formed with a hollow channel. The gelation process was an instantaneous chemical reaction as the crosslinker ions binding the hydrogel chains together. The penetration of crosslinker ions in hydrogel solution depends on the concentration of crosslinker ions, diffusion time, and the kinetics of crosslinking [22]. As soon as materials were dispensed from the coaxial nozzle tip, the microfluidic channel formed. The hydrogel solution dispensed from the outer tube was crosslinked and became the gel shell, where crosslinker flow through the inner part formed the hollow core.

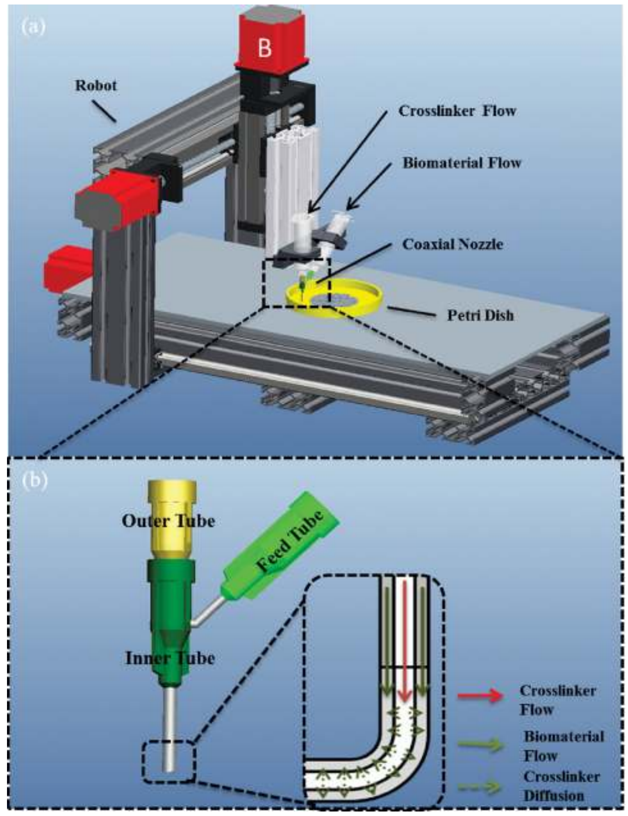

Fig. 1 A representative image of (*a*) the experimental setup and (*b*) coaxial nozzle assembly with fluid flow paths for hydrogel and crosslinker solutions. The coaxial system consists of three parts: inner tube, feed tube and outer tube.

2.4 Media Perfusion System. To test media transportation and perfusion capability of microfluidic channels, a customized system was developed. Figure 2 demonstrates the experimental perfusion system in a tissue culture incubator (Panasonic Healthcare Company of North America, IL). It consisted of a compact digital fluid pump (Cole-Parmer, IL) to provide media flow, a culture media reservoir with 1 l capacity, and an X-Y-Z axis motion stage (Edmund Optics, NJ) to facilitate precise positioning and alignment of nozzle tip. Medical-grade tubes (PharMed, OH) were used to connect the three main components of the perfusion system. 22 gauge flexible nozzle tips (Nordson, OH) were used to connect the microfluidic channels with the tubing system, and micro vessel clips were used to prevent leakage at the connection. Cell culture media was aspirated by the digital pump from the media reservoir and transported into a single microfluidic channel and then cycled back to the reservoir.

2.5 Cell Viability Analysis. Immediately after bioprinting, samples were kept in Hanks balanced salt solution (HBSS)

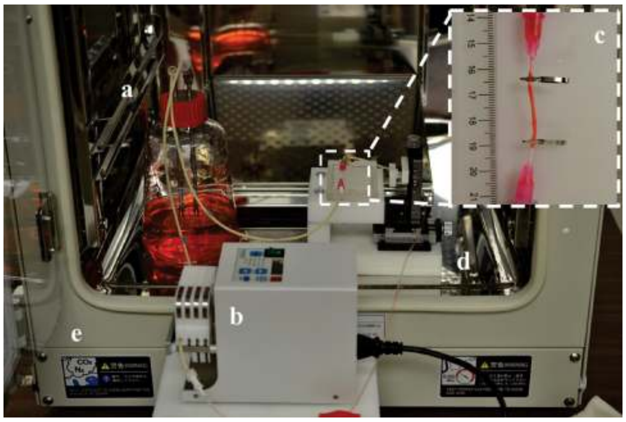

Fig. 2 Media perfusion system in an incubator: (*a*) culture media reservoir with capacity of 1 l, (*b*) digital pump, (*c*) media perfused cellular microfluidic channel; (*d*) three-axis motion stages, and (*e*) cell and tissue culture incubator

(InvitrogenTM Life Technologies, Carlsbad, CA) supplemented with 4% (w/v) calcium chloride to maintain crosslinking. Samples were washed with HBSS supplemented with 100 U/ml penicillin, 100 μg/ml streptomycin, and 2.5 μg/ml fungizone for sterilization before incubation. After washing, cellular microfluidic channels were cultured with perfusion system at 37 °C in 5% CO_2. Microfluidic channels, 10–15 cm in length, were cultured in a customized T-75 culture flask with perfusion of DMEM-base cell culture media through microfluidic channels. The flow rate was set at 10 ml/hour for 12-h continuous pumping. Cell viability assays were performed immediately after culturing to evaluate cell survival in response to media perfusion and perfusion-induced mechanical stimulation. 5 cm long microfluidic channels were printed for each sample, and three samples were used for each experimental group ($n = 3$). For cell viability analysis, samples underwent fluorescent microscopic examination. Microfluidic channels were stained with calcium acetoxymethylester (calcein AM) and ethidiumhomodimer-2 (Invitrogen) at a concentration of 1.0 mM each. Calcein AM is metabolized in living cells to form a bright green fluorescent product that accumulates in the cytosol. Ethidium homodimer is a red fluorophore that stains the DNA of nonviable cells but cannot penetrate living cells with intact plasma membranes. The staining medium was aspirated, and new medium was added to wash off any residual stains on the microfluidic channel surface before fluorescent illumination. After a 30-min incubation period, microfluidic channels were imaged under a Leica fluorescent microscope (Leica Microsystems Inc., Buffalo Grove, IL). Images were collected from three different locations randomly chosen from each sample. ImageJ (National Institutes of Health, Bethesda, MD) was used for automated counting of red- and green-stained CPCs in each image, and percentages of viable cells were calculated. The percentage of viable cells for each sample was calculated by averaging the values of three different locations.

2.6 Embedding Microfluidic Channels in Bulk Hydrogels. For embedding microfluidic channels in bulk hydrogels, microfluidic channels were printed directly into calcium chloride pools in petri dishes and soaked in the solution for over 30 min until they became fully crosslinked. During the crosslinking process, another petri dish was prepared and coated with 3–5 mm 4% alginate solution on the bottom. A coated petri dish was then fixed onto a horizontal shaker and underwent 3–5 min of shaking to get a uniform distribution with a flat surface. Completely crosslinked microfluidic channels were then aligned on top of the alginate-coated petri dish to get a zigzag pattern with arc turns. Another layer of alginate solution was then slowly pulled onto patterned microfluidic channels without introducing any air bubbles or clearance between layers. A horizontal shaker was also used here to ensure an even surface for the second layer. 4% calcium chloride solution was then carefully sprayed onto the petri dish to cover the whole surface of the alginate. The entire structure was merged in a calcium chloride solution until gelation was fully completed, after which microfluidic channels were embedded into bulk alginate gel. Similar procedures were used to embed alginate microfluidic channels by 3% chitosan and 1.0 M sodium hydroxide as crosslinking solution. Microfluidic channel embedded in bulk constructs were then used for media transportation and perfusion tests. Media with food dye was pumped through our perfusion system both for single-layer and multilayer microfluidic channels to show their functionality further.

2.7 Statistical Analysis. In Secs. 3.2 and 3.3, more than 50 pieces of data were obtained by measuring different microfluidic channels and different sections of printed microfluidic channels under a digital microscope (Motic®, BA310, Motic Incorporation Inc., Canada). The data shown in this paper were an average of all 50 pieces of data. The statistical analysis was carried out using Minitab 16. For all data, normality and independent tests were performed to ensure the data used for statistical significance analysis follow the required test assumption. The statistical difference analysis among groups was conducted by analysis of variance. Groups with a significance level of $p < 0.05$ were considered as significant.

3 Results and Discussions

3.1 Fabrication of Microfluidic Channels. The fabricated alginate and chitosan-microfluidic channels are shown in Fig. 3. Alginate microfluidic channels had relatively better mechanical and structural integrity compared to that of chitosan. The fabricated alginate microfluidic channels were continuous and had uniform diameter (see Fig. 3(*a*)). As shown in Fig. 3(*b*), although

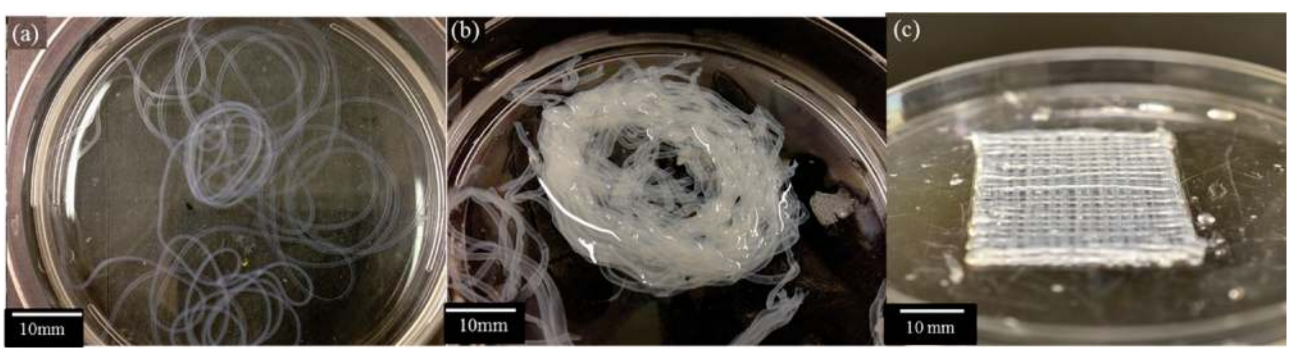

Fig. 3 Printed microfluidic channels: (*a*) alginate microfluidic channels have acceptable mechanical strength and structural integrity, (*b*) chitosan-microfluidic channels are fragile and easy to rupture, and (*c*) printed eight-layer alginate microfluidic channel network with well-defined morphology

uniform chitosan-microfluidic channels were obtained, their structural integrity was limited so that they were fragile and ruptured easily. The proposed fabrication platform was also capable of fabricating construct with 3D complex architecture. Fabrication was performed with 4% alginate solution with a dispensing rate of 0.2 ml/min, which demonstrated acceptable cell viability and good structural integrity. 4% calcium chloride solution was used as the crosslinker, which was dispensed at 1.5 ml/min. Figure 3(*c*) shows an eight-layer alginate microfluidic channel printed by the robotic system, which demonstrates the effectiveness of the fabrication platform.

3.2 Effect of Biomaterial Concentration on Microfluidic Channel Dimensions. In this study, hydrogels including chitosan and alginate were explored to determine their fabrication feasibility. In the first experiment, 2%, 2.5%, 3% and 4% chitosan solutions were prepared to print microfluidic channels. 1.0 M sodium hydroxide was used to crosslink the chitosan solution. However, only 2.5% and 3% chitosan were feasible to fabricate structurally well-integrated microfluidic channels with the selected fabrication parameters. The mechanical integrity of 2% chitosan was weak; the microfluidic channel snapped before a uniform channel formed. The viscosity of 4% chitosan was too high to be dispensed from the coaxial nozzle. Possibly, a higher dispensing pressure could allow ejecting the high viscous solution but this could induce considerable shear stress reducing cell viability [1]. Thus, Fig. 4(*a*) shows microfluidic dimension data obtained from microfluidic channels with 2.5% and 3% solution concentration. As chitosan concentration increased, microfluidic channel and core diameters as well as wall thickness decreased given the same dispensing pressure; however, more levels are required to perform a trend analysis. Figure 4(*b*) shows effect of alginate concentration on microfluidic channel dimensions. In this study, 3%, 4%, 5%, and 6% alginate and 4% $CaCl_2$ were used to fabricate microfluidic channels. In general, alginate with a solution concentration greater than 6% demonstrated limited cell viability and not recommended for cell encapsulation experiments [23]. The 4% alginate group had the smallest microfluidic dimensions including the core and the channel diameter as well as the wall thickness. The results in Fig. 4(*b*) revealed that there was no distinct trend between alginate concentration and filament dimensions. Indeed, the dimensions of printed microfluidic channels were primarily affected by the diffusion rate of Ca^{2+} ions, which was a function of alginate concentration and the thickness of the alginate ejected from the coaxial nozzle. In other words, alginate concentration affected the diffusion rate of Ca^{2+} ions as well as the thickness of the hollow filament ejected from the nozzle per the fixed dispensing pressure.

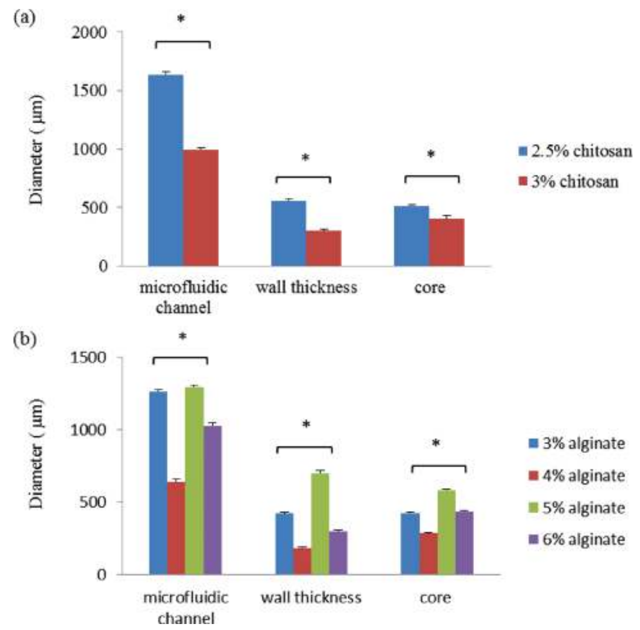

Fig. 4 Geometric comparison of printed microfluidic channels per variation in hydrogel concentrations including: (*a*) chitosan, and (*b*) alginate (single asterisk (*) indicates significant differences between groups ($p<0.05$))

Similarly, the concentration of $CaCl_2$ also had an effect on fabricated microfluidic channel diameter [24]. For example, Fig. 5(*a*) shows partially crosslinked alginate microfluidic channel which was fabricated with 4% alginate and 2% $CaCl_2$. This can be explained by gelation process, which depends on crosslinker and alginate concentrations as well as the flow rate of crosslinker through the core section. Due to low Ca^{2+} concentration in 2% $CaCl_2$ solution, only a small portion of the deposited alginate was crosslinked. This could be alleviated by increasing the concentration of $CaCl_2$. The wall thickness of microfluidic channels is critical for their functionality in both delivering perfused media through the core and allowing its diffusion for viability of encapsulated cells. The diffusion limit for hydrogels is around 200 μm [25,26], which indicates that if the wall thickness of fabricated microfluidic channel is smaller than 200 μm, there is a high chance of cell viability. However, smaller wall thickness is not always desirable. Mechanical and structural integrity of microfluidic channel decreases as the wall thickness decreases. Figure 5(*b*)

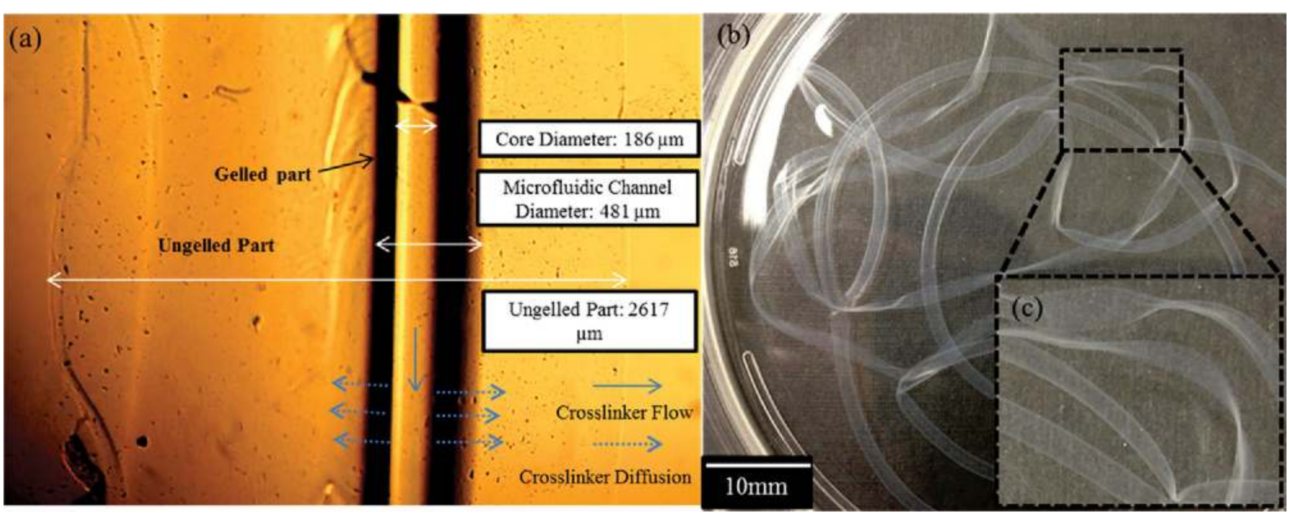

Fig. 5 (*a*) Partially crosslinked alginate (*b*) and (*c*) relatively weak structure bent and collapsed due to small wall thickness

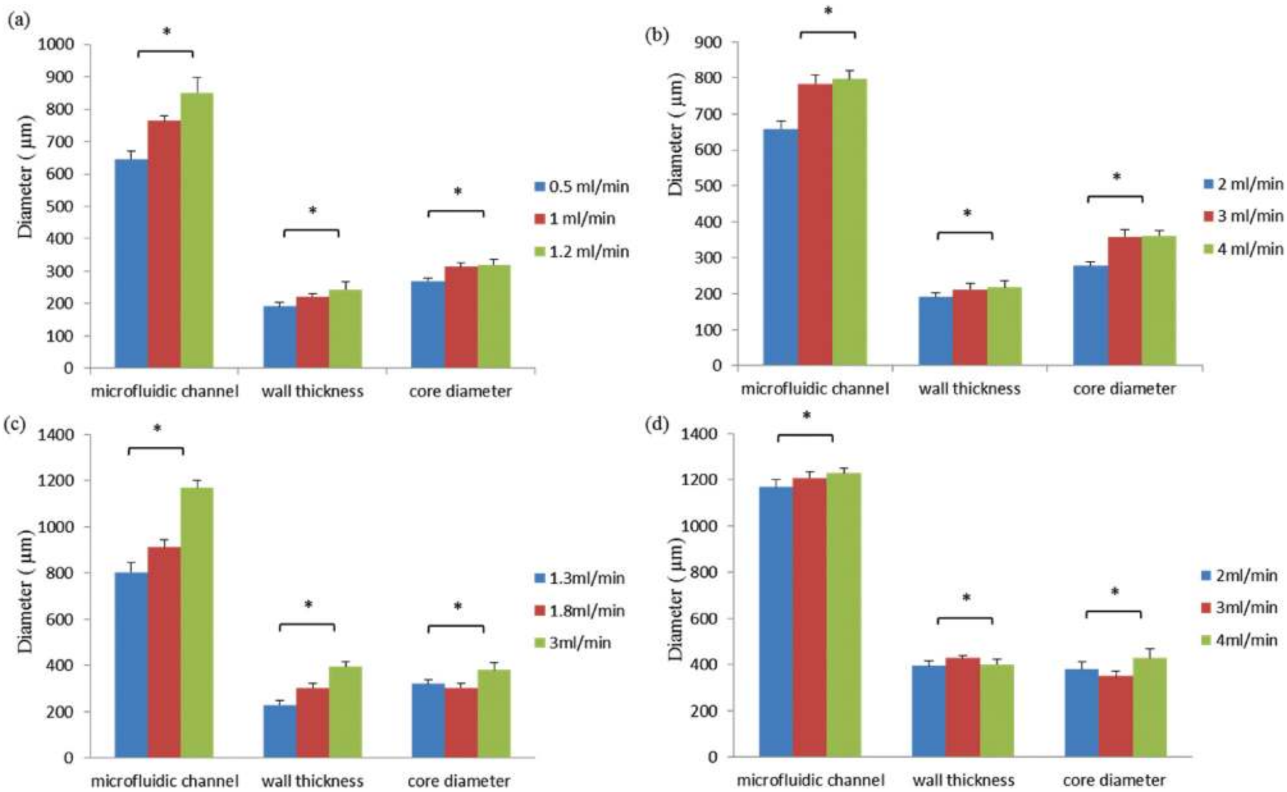

Fig. 6 Effect of flow rheology on the geometry of microfluidic channels: varying (*a*) alginate dispensing rate, (*b*) $CaCl_2$ dispensing rate, (*c*) chitosan dispensing rate, and (*d*) sodium hydroxide dispensing rate (single asterisk (*) indicates significant differences between groups ($p < 0.05$))

illustrates a microfluidic channel with thin wall, in which the channel was collapsed at several locations due to weak mechanical integrity.

3.3 Effects of Dispensing Parameters on Microfluidic Channel Dimensions. In this experiment, effects of dispensing parameters on microfluidic channel dimensions were studied. 4% alginate and 4% $CaCl_2$ were used to fabricate alginate microfluidic channels, and 3% chitosan and 1.0 M sodium hydroxide were used to fabricate chitosan-microfluidic channels. Alginate dispensing pressure, $CaCl_2$ dispensing rate, chitosan dispensing pressure and sodium hydroxide dispensing rate were varied to understand the effect of dispensing rates on microfluidic channel dimensions. Figure 6 illustrates the effect of abovementioned parameters on microfluidic channel dimensions. Microfluidic channel diameter increased as biomaterial or crosslinker dispensing rates increased. Increasing biomaterial dispensing rate resulted in greater volume of biomaterial dispensed per unit time generating enlarged microfluidic channels. This also brought thicker walls during extrusion (see Figs. 6(*a*)–6(*c*)). Increasing crosslinker flow rate generated more tension on channel wall in radial direction expanding the channels in cross-sectional profile that increased both core and channel diameter. No direct relationship was observed between wall thickness and the crosslinker flow rate (see Figs. 6(*b*)–6(*d*)).

3.4 Media Perfusion and Cell Viability Upon Perfusion. Figure 7(*a*) illustrates oxygenized media perfusion through an alginate microfluidic channel pattern 44 cm in length and 1 mm in width with 500 μm lumen diameter. The cell culture media was circulated through the channel with relatively low Reynolds number without any blockage and swirling that shows a great potential for developing embedded channels serving as a vascular network for thick tissue fabrication. Direct printing of these channels allows them to be integrated within a hybrid bioprinting platform and also facilitates patterning them into very complex shapes. Figure 7(*b*) shows the media flow with intentionally generated air bubbles under the digital microscope. The bubble was moving along the media flow. Cells were encapsulated in the hydrogel solution during the printing process and uniformly distributed in printed microfluidic channel (see Fig. 7(*c*)). The fluorescent microscope image showed quantifiable dead cells under live/dead cell staining (see Fig. 7(*d*)), but further quantifiable investigation of cell viability under media perfusion culture showed most of the cells were viable along the whole length of printed microfluidic channels. Figure 7(*e*) showed that average cell viability was $62.7 \pm 0.05\%$ after 12 h media perfusion postprinting. The diffusion of cell culture media was only realized through the internal surface of channels while the microfluidic channels proposed in thus study will later be embedded in cell-laden hydrogels as vascular networks; however, introducing the oxygenized cell media exogenously such as immersing the microfluidic channels inside the media during perfusion could support cell viability further. Neither leakage nor breakage was observed during perfusion of the media; however, some media permeated across the channel wall due to the permeability of hydrogel. 1.55 ml media was permeated on an 8 cm length channel at a perfusion rate of 30 ml/min in 3 h. The fabricated channel had acceptable mechanical properties as well. The elongation of channel due to perfusion was 0.4 cm.

3.5 Microfluidic Channels Embedded in Hydrogels. Alginate microfluidic channels were prepared and embedded in both bulk chitosan and alginate. Media with different color food dye was used to visualize fluid flow. When embedded in 4% alginate, microfluidic channels displayed a well-oriented pattern and structural integrity. It also transported media without blockage or disturbance (see Fig. 8(*a*)). Multidirectional media perfusion flow through two layers of alginate microfluidic channels was also

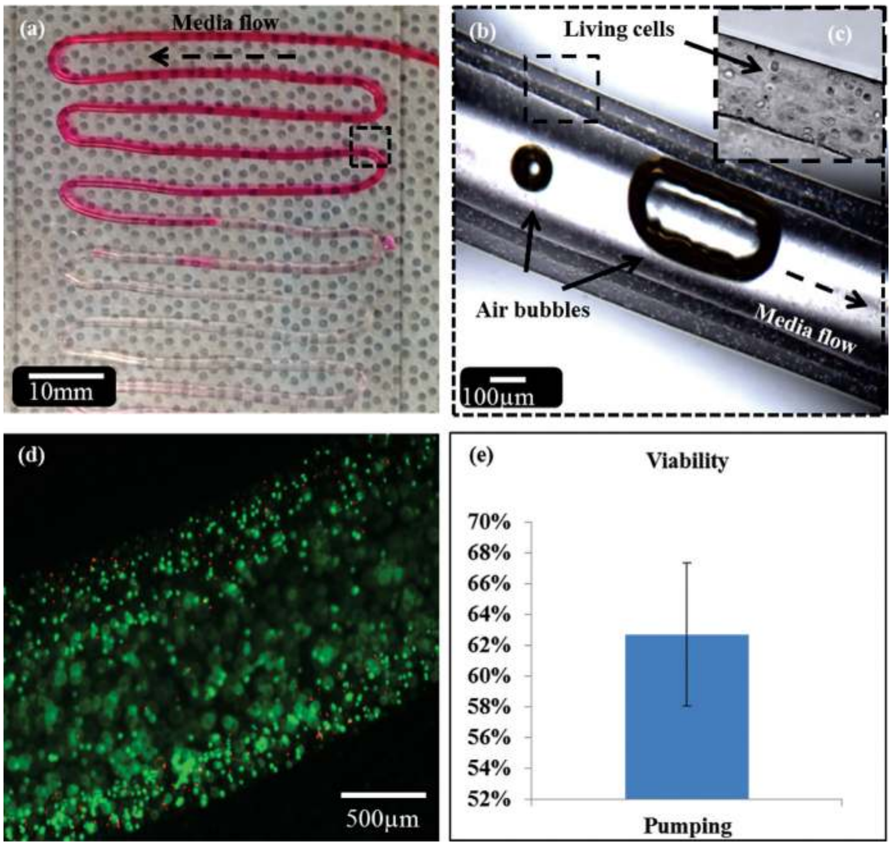

Fig. 7 Media perfusion and cell viability analysis: (*a*) perfusion of cell culture media through zigzag patterned channel showed no blockage or disturbance; (*b*) intentionally generated air bubbles illustrate media flow through the hollow feature of printed channels; (*c*) cells were uniformly distributed throughout the channel wall; (*d*) quantifiable cell death was observed along the microfluidic channel, but most of the cells were viable; (*e*) cell viability was around 62.7 ± 0.05% after 12 h of media perfusion

Fig. 8 Embedding microfluidic channels in bulk hydrogels. (*a*) alginate microfluidic channel embedded in bulk alginate displayed well-defined structure, and was able to transport media smoothly without any swirling formation (arrows indicate media flow direction); (*b*) two layers of alginate channels with multidirectional media perfusion (flow) (with red and green food dye); (*c*) alginate microfluidic channel embedded in bulk chitosan displayed well-defined pattern but ruptures were observed at respective locations along channels (circled sections), and (*d*) chitosan-microfluidic structure failed to transport media smoothly due to disrupted channels.

successfully performed (see Fig. 8(*b*)), indicating its potential to be integrated into thick tissue fabrication, serving as a vascular network. However, when embedded into chitosan hydrogel, alginate microfluidic channels showed rupture, especially at the turning point (see Fig. 8(*c*)). Also, it failed to transport media smoothly, and leakage was observed at the start point of perfusion (see Fig. 8(*d*)). In general, mechanical loading induced by the weight of bulk hydrogels affected structural morphology of microfluidic channels by collapsing them at respective locations. This could be, however, reduced by improving mechanical properties of microfluidic channels such as using optimum fabrication parameters or reinforcing nanofibers. Experiments showed that microfluidic channels (7 cm in length), which had been soaked in 0.5% calcium chloride solution for 5 h after fabrication, had 5.65 ± 1.78 kPa maximum tensile stress with 5.91 ± 1.12 kPa Young's modulus.

4 Conclusion

In this paper, a novel fabrication method is presented for the fabrication of printable vessel-like microfluidic channels. The system can be used for various biomaterials showing the versatility of the process. Alginate and chitosan in various concentrations were printed to fabricate microfluidic channels in broad range of dimensions with a wall thickness less than 200 μm. Results show that the hydrogel solution type and hydrogel solution concentration had great effects on microfluidic channel dimensions. Experiments were performed to explore the effects of dispensing parameters on printed microfluidic channel dimensions. Printed microfluidic channels were also able to support media transportation and perfusion either in form of individual channels or those embedded in bulk hydrogels to support cell viability.

As future work, nanofibers fabricated using electrospinning process will be reinforced into microfluidic channels to enhance their mechanical strength, structural integrity and functionality in bulk cell-laden hydrogels. Furthermore, a tri-axial nozzle assembly will be developed to fabricate microfluidic channels with two layers of concentric walls. Smooth muscle cells together with endothelial cells will be encapsulated in the outer wall and the inner wall, respectively, to develop natural blood vessels biomimetically.

Acknowledgment

This research has been supported by the National Institutes of Health (NIH) and the Institute for Clinical and Translational Science (ICTS) Grant No. ULIRR024979. The author also acknowledges the support from the Biological Science Funding Program (BSFP) at The University of Iowa. The authors would like to thank Dr. Edward Sander (Biomedical Engineering Department, The University of Iowa) for mechanical testing.

References

[1] Ozbolat, I. T., and Yu, Y., 2013, "Bioprinting Towards Organ Fabrication: Challenges and Future Trends," IEEE Trans. Biomed. Eng., **60**(3), pp. 1–9.
[2] Lee, W., Lee, V., Polio, S., Keegan, P., Lee, J. H., Fischer, K., and Park, J. K., Yoo SS., 2010, "On-Demand Three-Dimensional Freeform Fabrication of Multi-Layered Hydrogel Scaffold With Fluidic Channels," Biotechnol. Bioeng., **105**(6), pp. 1178–1186.
[3] Ling, Y., Rubin, J., Deng, Y., Huang, C., Demirci, U., Karp, J. M., and Khademhosseini, A., 2007, "A Cell-Laden Microfluidic Hydrogel," Lab Chip, **7**(6), pp. 756–762.
[4] Cuchiara, M. P., Allen, A. C. B., Chen, T. M., Miller, J. S., West, J. L., 2010, "Multilayer Microfluidic PEGDA Hydrogels," Biomaterials, **31**(21), pp. 5491–5497.
[5] Golden, A. P., and Tien, J., 2007, "Fabrication of Microfluidic Hydrogels Using Molded Gelatin as a Sacrificial Element," Lab Chip, **7**(6), pp. 720–725.
[6] Offra, S.-N., Noga, L., Ruthy, Z., Shy, S., and Dror, S., 2009, "Laser Photoablation of Guidance Microchannels Into Hydrogels Directs Cell Growth in Three Dimensions," Biophys J., **96**(11), pp. 4743–4752.
[7] Chan, V., lutuna, P., Jeong, J. H., Kong, H., and Bashir, R., 2010, "Three-Dimensional Photopatterning of Hydrogels Using Stereolithography for Long-Term Cell Encapsulation," Lab Chip., **10**(16), pp. 2062–2070.
[8] Lee, S.-H., Moon, J. J., and West, J. L., 2008, "Three-Dimensional Micropatterning of Bioactive Hydrogels Via Two-Photon Laser Scanning Photolithography for Guided 3D Cell Migration," Hydrogel Solutions, **29**(20), pp. 2962–2968.
[9] Wang, L., Kodzius, R., Yi, X., Li, S., Hui, Y. S., Wen, W., 2012, "Prototyping Chips in Minutes: Direct Laser Plotting (DLP) of Functional Microfluidic Structures," Sens. Actuators B, **168**(0), pp. 214–222.
[10] Hnatovsky, C., Taylor, R. S., Simova, E., Bhardwaj, V. R., Rayner, D. M., Corkum, P. B., 2005, "Polarization-Selective Etching in Femtosecond Laser-Assisted Microfluidic Channel Fabrication in Fused Silica," Opt. Lett., **30**(14), pp. 1867–1869.
[11] Zheng, Y., Henderson, P. W., Choi, N. W., Bonassar, L. J., Spector, J. A., and Stroock, A. D., 2011, "Microstructured Templates for Directed Growth and Vascularization of Soft Tissue *In Vivo*," Biomaterials, **32**(23), pp. 5391–5401.
[12] Nazhat, S. N., Neel, E. A., Kidane, A., Ahmed, I., Hope, C., Kershaw, M., Lee, P. D., Stride, E., Saffari, N., Knowles, J. C., and Brown, R. A., 2006, "Controlled Microchannelling in Dense Collagen Scaffolds by Soluble Phosphate Glass Fibers," Biomacromolecules, **8**(2), pp. 543–551.
[13] Kim, D.-N., Lee, W., and Koh, W.-G., 2008, "Micropatterning of Proteins on the Surface of Three-Dimensional Poly(Ethylene Glycol) Hydrogel Microstructures," Anal Chim. Acta, **609**(1), pp. 59–65.
[14] Liu, S., Xiong, Z., Wang, X., Yan, Y., Liu, H., and Zhang, R., 2009, "Direct Fabrication of a Hybrid Cell/Hydrogel Construct by a Double-Nozzle Assembling Technology," J. Bioactive Compat. Polym., **24**(3), pp. 249–265.
[15] Skardal, A., Zhang, J., and Prestwich, G. D., 2010, "Bioprinting Vessel-Like Constructs Using Hyaluronan Hydrogels Crosslinked With Tetrahedral Polyethylene Glycol Tetracrylates," Biomaterials, **31**(24), pp. 6173–6181.
[16] Landers, R., Hubner, U., Schmelzeisen, R., and Mulhaupt, R., 2002, "Rapid Prototyping of Scaffolds Derived From Thermoreversible Hydrogels and Tailored for Applications in Tissue Engineering," Biomaterials, **23**(23), pp. 4437–4447.
[17] Roth, E. A., Xu, T., Das, M., Gregory, C., Hickman, J. J., and Boland, T., 2004, "Inkjet Printing for High-Throughput Cell Patterning," Biomaterials, **25**(17), pp. 3707–3715.
[18] Cheah, C. M., Chua, C. K., Leong, K. F., Cheong, C. H., and Naing, M. W., 2004, "Automatic Algorithm for Generating Complex Polyhedral Scaffold Structures for Tissue Engineering," Tissue Eng., **10**, pp. 595–610.
[19] Fang, Z., Starly, B., and Sun, W., 2005, "Computer-Aided Characterization for Effective Mechanical Properties of Porous Tissue Scaffolds," Comput.-Aided Des., **37**(1), pp. 65–72.
[20] Zhao, L., Lee, V. K., Yoo, S. S., Dai, G., and Intes, X., 2012, "The Integration of 3-D Cell Printing and Mesoscopic Fluorescence Molecular Tomography of Vascular Constructs Within Thick Hydrogel Scaffolds," Biomaterials, **33**(21), pp. 5325–5332.
[21] Yu, Y., 2012, "Identification and Characterization of Cartilage Progenitor Cells by Single Cell Sorting and Cloning," M.S. thesis, University of Iowa, Iowa City, IA.
[22] Shin, S.-J., Park, J.-Y., Lee, J.-Y., Park, H., Park, Y.-D., Lee, K.-B., Whang, C.-M., and Lee, S.-H., 2007, ""On the Fly" Continuous Generation of Alginate Fibers Using a Microfluidic Device," Langmuir, **23**(17), pp. 9104–9108.
[23] Bohari, S. P., Hukins, D. W., and Grover, L. M., 2011, "Effect of Calcium Alginate Concentration on Viability and Proliferation of Encapsulated Fibroblasts," Biomed. Mater. Eng., **21**(3), pp. 159–170.
[24] Zhang, Y., Yu, Y., Chen, H., and Ozbolat, I. T., 2013," Characterization of Printable Cellular Micro-Fluidic Channels for Tissue Engineering," Biofabrication, **5**(2), p. 024004.
[25] Malda, J., Klein, T. J., and Upton, Z., 2007, "The Roles of Hypoxia in the *In Vitro* Engineering of Tissues," Tissue Eng., **13**(9), pp. 2153–2162.
[26] Rouwkema, J., Rivron, N. C., and van Blitterswijk, C. A., 2008, "Vascularization in Tissue Engineering," Trends Biotechnol., **26**(8), pp. 434–441.